CARBONATES AND OTHER SALTS IN THE ATACAMA DESERT AND ON MARS, AND THE IMPLICATIONS FOR THE ROLE OF LIFE IN CARBONATE FORMATION

by

Patrick L. Harner

A Thesis Submitted to the Faculty of the

DEPARTMENT OF PLANETARY SCIENCES

In Partial Fulfillment of the Requirements

For the Degree of

MASTER OF SCIENCE

In the Graduate College

THE UNIVERSITY OF ARIZONA

2015

STATEMENT BY AUTHOR

This thesis has been submitted in partial fulfillment of requirements for an advanced degree at the University of Arizona and is deposited in the University Library to be made available to borrowers under rules of the Library.

Brief quotations from this thesis are allowable without special permission, provided that an accurate acknowledgement of the source is made. Requests for permission for extended quotation from or reproduction of this manuscript in whole or in part may be granted by the head of the major department or the Dean of the Graduate College when in his or her judgment the proposed use of the material is in the interests of scholarship. In all other instances, however, permission must be obtained from the author.

SIGNED: Patrick L. Harner

Patrick L. Harner

APPROVAL BY THESIS DIRECTORS

This thesis has been approved on the date shown below:

Jay Quade
Jay Quade
Professor of Geology

May 5th 2015
Date

Victor Baker
Victor Baker
Professor of Lunar and Planetary Science

May 5th 2015
Date

ACKNOWLEDGEMENTS

I would like to acknowledge the contributions to this thesis of Drs. Jay Quade, Julie Neilson, and Audrey Copeland for their in-field analysis of plant cover, site description, and sample collection. In addition, I thank J. Gregory Caporaso and William van Treuren for their roles in sample collection, funded by the Lewis and Clark Fund for Exploration and Field Research in Astrobiology.

Dr. Quade made all qualitative carbonate estimations and non-soil pit isotopic measurements displayed in Fig 2 and 5. Additionally, he has compiled the age data, soil descriptions, and climate data displayed in Table 1, and made significant contributions to the development of this document throughout its several iterations. This contribution was supported by National Geographic and the NSF. Dr. Neilson has provided all of the non-carbonate salt data for the soil transects, as well as organic matter content used within the carbonate model, which was funded by the National Science Foundation Microbial Observatory grant MCB0604300.

TABLE OF CONTENTS

LIST OF FIGURES/ILLUSTRATIONS AND TABLES

ABSTRACT

The scarcity of carbonate on Mars has been difficult to reconcile with the morphologic evidence for a wet epoch in Martian history, and has weakened early interpretations of a water-rich Noachian. Limited soil carbonate from pre-Silurian Earth has created a similar conundrum, and in both instances this paradox has likely led to overreaching interpretations about past climates. To better understand the formation of carbonate on Mars, early Earth, and in present day hyperarid climates, we examined the distribution of carbonate in the Atacama Desert—a region that spans multiple climate regimes and allows us to isolate the effects of precipitation and plant cover on soil mineralogy. To better quantify the influences of vegetation on carbonate we utilized a simple one-dimensional precipitation model and simulated carbonate formation with or without plant cover under a range of relevant climatic conditions and soil morphologies.

In the Atacama we found two distinct zones with only trace (<5%) carbonate: the "absolute desert" with precipitation too low to sustain plant life, and the high Andes where precipitation was significantly higher, but where the low mean annual temperature (MAT) inhibits plants. The fog-supported, low-elevation coastal "lomas" below approximately 800 meters above sea level (masl) and the higher elevations between approximately 2500-4500 masl are variably vegetated and contain abundant carbonate within the soils. Plants increase total evapotranspiration and its distribution with depth, weathering rates, and total pCO_2. Our model results show that all of these factors increase the formation of pedogenic soil carbonate. Without the influence of vegetation the diminished carbonate that is produced is flushed through the shallow soil, where it eventually precipitates in the deep vadose zone or is entrained by groundwater.

BACKGROUND AND MOTIVATION

The Carbonate Paradox on Mars

This study was motivated by a desire to understand the processes that control the distribution of salts, with a focus on carbonate salts, under the hyperarid surface conditions experienced by the Atacama Desert of west-central South America, and which are similar to those conditions predicted for the majority of Mars's history. The surface environments of both the Atacama and Mars are characterized by a hyperarid, unvegetated climate, and both surfaces host abundant soluble salts, but strikingly sparse carbonates. The Atacama allows us to investigate the weathering conditions present on a surface with no plants and little precipitation, and provide insight into what effect the presence or absence of life has on carbonate formation.

The sparsity of carbonate on Mars presents a conundrum. Abundant morphologic evidence points to a Noachian climate with at least periods of standing surface water and significantly warmer surface conditions than observed on present-day Mars (Carr, 1996). Any sustained warmer and wetter Martian climate would require a strong greenhouse effect, and climate models for early Mars have relied upon a thick, dominantly CO_2 atmosphere to provide the necessary warming (e.g. Pollack et al., 1987). While research into Mars's early climate is active and ongoing, the general lack of carbonate found on the surface remains one of the largest difficulties in ascribing an early CO_2-rich atmosphere to Mars.

Despite the lack of demonstrably pedogenic soil carbonate on the surface of Mars, there is evidence for a small homogenous fraction of carbonate within the soil, similar to what we have documented in the Atacama Desert. Early Earth-based infrared spectral observations detected a small fraction (<5%) of carbonate within the relatively ubiquitous dust cover (e.g. Blaney and McCord, 1989; Calvin et al., 1994). Later observations made with the Thermal Emissions

Spectrometer (TES) orbital data confirmed a 3-5%, likely magnesite-rich, global carbonate fraction in dust (Bandfield et al., 2003). Direct detection methods by rovers have often had a difficult time distinguishing low levels of carbonate from atmospheric carbon, but they have been able to place an upper limit for carbonate of only a few percent (Toulmin et al., 1977; Clark and Hart, 1981; Christensen et al., 2004). The Phoenix lander detected 3-6% calcium carbonate in the soil, exposed by Heimdall Crater within the last 500 Ma (Smith et al., 2009; Boynton et al., 2009), either from antecedent material exhumed by the impact, or as re-precipitations of pedogenic soil carbonate. The Curiosity rover has also detected low abundances of carbonate (Leshin et al., 2013), but well within the few percent maximum range established by previous missions.

The Atacama Desert of northern Chile and southern Peru is one of the driest places on Earth, and it is a logical place to try to understand the formation processes of carbonate in a hyperarid setting comparable to Mars. Previous studies analyzing the Atacama's unique salt assemblages have offered insights into the origin and detectability of perchlorate, sulfate, and nitrate on Mars (e.g. Navarro-Gonzalez et al., 2003; Catling 2010; Michalski et al., 2004). In this paper we present the results of a comprehensive effort to characterize soils and their salts, including carbonate, along transects spanning the gradient seen in the Atacama (Fig. 1, 2) from the absolute desert into the vegetated fog layer, and finally into the wetter high Andes, too cold for vegetation (Fig. 3). To understand the distribution of carbonate in Atacama soils, we adapted a soil model based on 1D carbonate-balance models previously developed for and applied to carbonate-based paleoclimatology (Mayer, 1988). This model, among other things, allows us to predict the distribution of carbonate with soil depth in the presence or absence of plant cover, the

results of which can ultimately be compared to observed carbonate distributions in the Atacama and on Mars.

The Atacama Desert

The Atacama Desert spans the Pacific Coast of Chile and Peru from about 10 1, and is bordered by the Pacific Ocean on the west and the Andes to the east. For any given latitude, rainfall and plant cover vary regularly east to west and with elevation across the narrow desert (Fig. 2). Along the Pacific coast, a semi-permanent fog layer below ~1000 masl supports a unique and diverse Lomas "hill" shrubland (Rundel et al., 1991) (Fig. 3 C). To the east, a 100km wide hyperarid region with little measurable precipitation and no vegetation, referred to in this paper as the "absolute desert" extends from the Lomas shrubland below 1000 masl to 2500-3000 masl, depending on latitude (Fig 3 A). To the east of the absolute desert, moist air masses borne by the tropical easterlies cross the Bolivian Altiplano and occasionally lap over the Andes and rain out at higher elevations. From approximately 3200 to the 4000 masl, a region described as the Tolar zone, is dominated by C_3 shrubs (50-100 mm/yr mean annual precipitation (MAP)), and above this the high Andean steppe (4000-4500 masl; 100-200 mm/yr MAP) with some partial C_3 grass cover (Villagrán et al., 1981, 1983; Arroyo et al., 1988) (Fig 3 B). Plants fade as elevation increases and temperatures decrease; as the 0° isotherm is crossed, above 4500-5000 masl, plants disappear entirely.

Across the entire gradient, soil parent material is non-calcareous and mostly volcanic (Latorre et al., 2002; Quade et al., 2007). Numerous salt pans, "salars," dot the Atacama (Fig. 3 E, F), and the extreme hyperaridity of the absolute desert has led to a unique accumulation of soluble salts in both the salars and the surrounding soils. The salars appear to play a role as a

source of salt that is redistributed into surrounding desert soils (Bao et al., 2004; Rech et al., 2003).

METHODS

Laboratory Methods

Results for this study include hundreds of samples and observations obtained from several hundred field sites (Fig 1). From these sites, the presence or absence of visible soil carbonate cementation was noted on clasts in soil matrix, and the degree recorded according to the scheme of Gile et al. (1966). A handful of these samples have been analyzed for carbonate content. In addition, over 100 samples were taken from twenty-four soil pits along the Baquedano (BAQ) and Yungay (YUN) transects (Fig. 1), spanning from <1000 masl elevation in the absolute desert to >4500 masl above the vegetated zone. At each site five samples were extracted, at ten centimeter depth increments down to 50cm. Soil profile descriptions were created for each site.

For carbonate analysis, each sample was powdered and treated to remove organic carbon by adding 3mL of 3% H_2O_2 to ~1-3 grams of the sample. The mixture was then allowed to react and degas for 2-3 hours. Samples were then rinsed with distilled water and centrifuged three times, and placed within an 80°C oven for a minimum of two days to dry.

Laboratory carbonate percents were measured using standard gas extraction methods. Powdered samples were weighed and placed under vacuum at room temperature. Samples were then sealed and reacted with 100% phosphoric acid in a 50-70°C bath to speed the reaction. Through a series of cold-traps, CO_2 gas was isolated and a total carbon volume was recorded as a function of pressure. This total volume of carbon was related back to an overall mass percent,

making the assumption that all of the inorganic carbon within the soil was in the form of calcite; this assumption has been in previous analysis and is justified by the dominance of calcite within the region (Valdivia-Silva et al., 2012). Detection limits were determined by extrapolating the total volume necessary to induce a pressure reading above background to a carbonate percent based on the initial mass of the sample.

$\delta^{18}O$ and $\delta^{13}C$ isotopic measurements were obtained from a portion of the same sample analyzed for overall carbonate, after pretreatment of the whole sample. Samples were analyzed using an automated carbonate preparation device (KIEL-III) coupled to a gas-ratio mass spectrometer (Finnigan MAT 252) at the University of Arizona. Under vacuum at 70°C the samples were reacted to dehydrated phosphoric acid and the volatilized CO_2 gas from the reaction was then measured. Isotopic ratio measurements were calibrated based on NBS-19 standards. Results are presented in per mil (‰) delta (δ) notation, where $\delta = (R_{sample}/R_{PDB\ std} - 1)\cdot 1000$, and $R = {}^{13}C/{}^{12}C$.

Plant cover was estimated at each site using the log-series survey method developed by McAuliffe (1990). Non-carbonate salt data for Cl^-, SO_4^{2-}, NO_3^-, and PO_4^{3-} were measured using the Dionex ICS-1000 Ion Chromatography System with an AS22 anion exchange column at the University of Arizona.

The Soil Sites

The parent material, age, and geomorphic position of soils included in this study vary considerably, and here we offer some generalizations of these features for contextualization of our analytical results. In soils > 3000 masl, parent material is entirely volcanic rocks of various types, and their alluvial derivatives (Table 1). Below 3000 masl parent material is much more variable and includes volcanic rocks but also sedimentary rocks of mostly Mesozoic age.

Virtually all sedimentary rock is siliclastic; carbonate rocks are confined to a few rare occurrences of limestone and hydrothermal vein calcite.

Soil and land surface age are key considerations in soil development. In a few cases we evaluated age from the age of known parent material, but most soil ages were evaluated based on their degree or stage of carbonate accumulation after Gile et al. (1996). Soil carbonate cements typically evolve through a series of stages that takes 10^3 to 10^6 yrs to complete in gravelly soils. The process involves the accumulation of thin coats of carbonate on the underside of clasts (Stage I), more continuous coatings (Stage II) to eventual plugging of soils (Stage III) and development of a laminar cap (Stage IV).

Using these criteria, ages of soils <3000 masl are quite variable, from <10 ka, to as high as 10^6 yrs for a few cases (Table 1). By contrast, ages of soils tend to be young (<10,000 years) on most soils above 3000 masl, as evaluated from degree of soil development and from age of the local parent material. The relative youth of most high-elevation soils is the result of the steep and active topography, and abundant recent volcanic activity. For example, all of the soils in the upper Yungay transect (YUN 3259, 3346, 3428, 3533, 3856) are developed on loose cinder associated with the Socompa eruption <10,000 ka). Other sites such as BAQ 3473, 4166, and 4697 are also developed on young cinder or their very young alluvial derivatives (Fig. 3 B). Such soils were the focus of our detailed profile sampling, whereas a much broader age range of high elevation soils were inspected and analyzed for carbonate development and isotopic composition (Fig. 1).

Twenty-two soil pits were excavated to ~50 cm depth, described, and sampled at 10cm intervals for salts content. They were also sampled for microbes, which will be presented elsewhere. An additional three soils, Paposo 130, 425, and Soc 3371 were described and

sampled to several meters depth in natural exposures. In general, soils from the coastal lomas (Table 1; Paposo-130) are rocky alluvial fan soils with reddened and clay-rich B horizons and well-developed (Stage II-IV) calcic horizons (Fig. 3 C, D). The lomas sites are the most densely vegetated of all the sites (Table 1), with a mix of shrubs, succulents, and herbs.

Soils of the absolute desert 1000-2400 masl are developed on gravelly alluvium and capped by thick (5-15cm) loessic Av horizons. They completely lack the reddening in the upper B horizon and visible carbonate cementation in the lower part so characteristic of older alluvial soils in the lomas. Carbonate is often detectable as weak effervescence in the soil matrix. Dispersed to densely cemented gypsic horizons are typically present below ~20cm soil depth. All absolute desert sites are unvegetated (Fig. 3 A)

Soils in the transition zone to the higher, well-vegetated elevations (BAQ 2420, 2462, 2838, 2687; YUN 3153, 3259, 3346) are developed on young alluvium and show little soil development except the presence of loessic Av capping horizons. Weak (Stage I) calcic and gypsic horizons can be present. None of these sites were vegetated at the time of sampling but plants are present in nearby washes, and probably periodically grow on the sites judging from the presence of root hairs in some of the profiles such as BAQ 2420.

From 3400 to 4500 masl level sites are developed on volcanic cinder, ignimbrites, and their alluvial derivatives. Most show little profile development aside from the addition of loess to the top of the profile. Gypsum is rare at this elevation with YUN 3473 being the exception. Visible carbonate accumulation is observed on most soils developed on older alluvium (Table 1), reaching Stage III-IV on the oldest land forms (Fig. 3 D), but not evident on younger soils developed on loose cinder. Plant cover is shrubby Tolar at lower elevations (Fig. 3 B) and *Stipa-Festuca* grassland at higher elevations (4166 masl) (Fig. 3 C).

Finally, soils above 4600 masl are developed on a variety of volcanic rocks and show variable reddening in the upper part of profiles, but do not exhibit any salt accumulation of any kind at depth, despite development on open, stable surfaces. They are unvegetated except thinly on some north-facing slopes.

Carbonate Budget Model

To understand the impact of plant cover on pedogenic carbonate development in arid environments we utilize a simple model adapted from the CALSOIL 2.0 model (Mayer, 1988). Similar carbonate formation models have been successfully applied to predict formation age and climatic conditions of pedogenic carbonate accumulation (e.g. Marion et al., 1985; Mayer 1988; Hirmas et al., 2010). The CALSOIL model uses mass balance to account for water and carbonate flow along one-dimensional compartments of variable depth, assuming entirely top-down flow. As precipitation enters into a compartment it carries with it dissolved carbonate from previous layers, or from carbonate dust on the surface of the profile. Water can then dissolve additional carbonate and/or precipitate some of its existing inventory of dissolved carbonate as calcite. The model allows for a broad array of climatic and soil parameters as inputs that effectively control the amount and distribution at depth of carbonate that forms.

Our model was specifically adapted to isolate the influence of plants, and was parameterized to represent carbonate formation under either a complete absence of vegetation (NOPLANT) or a vegetated scenario (PLANT) typical of the Tolar zones of the Atacama at ~3500 masl. For PLANT this included: the addition of organic matter as a soil component; an adjustment to total monthly potential evapotranspiration and its distribution with depth; and an increased pCO_2 at depth, due to plant respiration (Quade et al., 2007).

The field capacity and wilting point of the soils, defined as the volume of water retained under 1/3 and 15 bars suction-pressure, respectively, were calculated from a representative soil morphology using equations by Rawls et al. (1982), with an included organic component in the vegetated case as mentioned above. Stony content, not included within the Rawls equations but influential in calcareous soils (Cousin et al., 2003), was incorporated into the water budget capacity term (Cazemier, et al., 2001). These models, particularly in water-limited terrains, have been demonstrated to be strongly influenced by the water holding capacity of a compartment (Marion et al., 1985), and therefore no other differences were included between PLANT and NOPLANT beyond the organic matter term.

Effective precipitation and carbonate dust cover were held constant between the two simulations, despite possible climatic variations indirectly related to plant cover. Full model details, including those functions used to derive specific parameters, and a detailed overview of all specific adaptations to CALSOIL 2.0, are included in supplement A.

RESULTS

With regard to both salt and isotopic composition, the soils of the BAQ and YUN transects fall into one of three basic zones, reflecting both climatic conditions and soil age (Tables 1, 2). The three zones are: the unvegetated absolute desert, the unvegetated very high elevations, and the vegetated coastal lomas and mid-elevations.

Non-Carbonate Salt Profiles in the Atacama

Soils from the absolute desert are characterized by very high sulfate, chlorine, and nitrate (Fig. 2, Table 2). These include BAQ895 to BAQ1552 and BAQ2838 in the Baquedano transect and YUN1005 to YUN3184 in the Yungay transect, and the abundance within these soils can be

several orders of magnitude higher than within the vegetated zones (Table 2). These salts tended to increase with depth, down to the base of the measured profiles at 40-50 cm, and are often 10-50 times higher at depth than at the 0-10 cm. The S/Cl ratio within the absolute desert is unusually high, averaging >20 mole fraction.

By contrast, sulfate, chlorine, and nitrate are very low in the wetter zones both where vegetation is present at the coastal lomas and mid-elevations, and where vegetation is not present at elevations >4500 masl. This high concentration of non-carbonate salts and the high S/Cl ratio diminish immediately at the transitional sites at the boundary of the absolute desert and adjoining vegetated zones (Table 2; BAQ2420-BAQ2462). Moreover the S/Cl ratio reduces to <1 in the areas where plant cover begins.

Phosphate, which was also measured, is low in all zones, often below the detection threshold. Phosphate does not display the same sharp contrasts with vegetation or predicted MAP that the more soluble salts do.

Carbonate in Atacama Soil

The qualitative presence or absence of visible soil carbonate showing Stage I or greater development was noted in a large range of sites (Fig. 5). In general these observations demonstrate a strong but not perfect coincidence of visible soil carbonate cementation with the presence of plants. For example, carbonate is abundantly and conspicuously present in older soils (Table 1, $>10^4$ yrs) in the coastal lomas zone (Fig. 3 D), and in the mid-elevation Tolar and steppe grass zones (Fig. 3 C). By contrast carbonate cements were not observed in soils of any age in the plantless absolute desert and high elevations (>4600 masl) zones. Carbonate cements are also not observed in young soils (Table 1, $<10^4$ yrs) of the plant-covered mid-elevation Tolar and steppe grass zones (Fig. 5).

Quantitative analysis from twenty-four soil profiles confirms these general patterns but also reveals the presence of carbonate in many (but not all) even where carbonate was not visible as a discrete cement. Within the Paposo130 soil pit taken within the vegetated coastal region, soil carbonate reached as high as 17%. The absolute desert is characterized by detectable but low percentages of carbonate (0-3%) (Fig. 4 A, B; Table 2). Field analysis describes all carbonate development within this zone as Stage I, and laboratory analysis for most profiles within the absolute desert sections places the carbonate fraction at 0-1%, although peak carbonate depths can reach 2-3%. This agrees with previous research that found inorganic carbonate formation limited to 0-5% in similar hyperarid Atacama soils (Drees et al., 2006; Prellwitz, 2007; Valdivia-Sylva et al., 2012).

Carbonate in the majority of profiles peaks within 30cm of the surface. Two sites, BAQ1370 and YUN3153 (Fig. 4 A), show an exponential decline in carbonate with depth, but the majority of the profiles have sharply lower carbonate at the surface, similar to what is seen with the other salts. YUN2029, which was positioned on an isolated hill, was anomalous in that it exceeded 5% carbonate between 40 and 50cm, while having no detectable carbonate within 30cm of the surface. This seems to correlate with other measured salts in the profile (Table 2).

A slightly different carbonate distribution is observed in transitional areas where plant cover is generally very low (<1%) and plants are only intermittently present during the year (Fig. 4; BAQ2420, BAQ2467). At BAQ2462 there was no evidence for surface vegetation but rootlets were abundant throughout the profile, likely representing seasonal or storm-runoff related plant life. In three transitional sites (BAQ2420-2687), carbonate exceeds 2.5% and is thicker throughout the profile than in those sites of the absolute desert (Fig. 4; Table 2). BAQ2687 has the highest peak carbonate abundance and its carbonate is the most concentrated

soil profile within this transitional zone. This concentration at the 20-30cm depth appears to correlate with a root that was observed within the same zone. Carbonate cementation has been observed to occur around root hairs (Kraimer and Monger, 2009; Monger et al., 2009) in other deserts. Many of the soil pits in the Tolar zone were from younger soils with little shallow soil carbonate, but a deeper soil pit taken within this zone from AD04-46 had three stages of carbonate, peaking as high as 26%.

$\delta^{13}C$ and $\delta^{18}O$ Isotopic Analysis of Soil Carbonate

Soils within the absolute desert tend to have $\delta^{13}C$ (PDB) values >+2‰ (Fig. 2, Table 2). BAQ1370 is the only substantial exception, where at depth it shows a $\delta^{13}C$ (PDB) value of -3‰ (Fig 4). In permanently or intermittently vegetated sites there is a systematic shift to lower values between -8 and 0‰ reflecting the influence of CO_2 derived from C_3 plants observed at these sites. $\delta^{13}C$ (PDB) values within the vegetated profiles also tend to decrease with depth, as observed in many desert profiles (Quade et al., 1990; Fig. 4). Many of the soil profiles taken from very young, higher elevation soils were too low in carbonate to allow for isotope analysis. Those profiles from older soils in this zone had $\delta^{13}C$ (PDB) values as low as -8‰ (Fig. 2). $\delta^{18}O$ (PDB) values, while more variable, ranged from -8 to +7‰, and tend to trend with $\delta^{13}C$ (PDB) values (Fig. 4, Table 2).

Model of Soil Carbonate Formation

Our modeling results show clear differences in the amount and distribution of resulting soil carbonate in the PLANT and NOPLANT experiments. Alterations to total evapotranspiration, the distribution of evapotranspiration with depth, and an increase in pCO_2 are all plant-related effects that tend to increase the abundance of soil carbonate. Each of these factors is dependent on plant species, plant health, and climate, and our simulation-pairs were

run over a range of reasonable values. Where plant cover was present, total carbonate accumulation across the profile was higher regardless of variations in other climate or morphologic parameters; the carbonate which formed was also typically concentrated into a single zone, or carbonate horizon (Fig. 6). NOPLANT simulations generated less total carbonate and typically accumulated carbonate in either an even distribution or one that mirrored the evaporation function with depth (Fig. 6). In those simulations where monthly evapotranspiration was periodically lower than monthly precipitation, the NOPLANT scenario was more likely to lose a substantial fraction to depth beneath the soil profile. In general there is good agreement between model results and what is observed within Atacama soil profiles (Fig. 4, Fig. 6).

We also examined the role of individual parameters within the model. The exponential accumulation of pCO_2 at depth has previously been demonstrated to increase carbonate solubility and lower the depth of carbonate accumulation. This effect was hypothesized to be countered by the plant-induced increase to evapotranspiration at depth (Marion et al., 1985). In our model the inclusion of even a minor pCO_2 increase with depth causes the peak accumulation depth to lower, but also shallows the maximum depth at which carbonate accumulates. As pCO_2 rises so does carbonate solubility, and the soluble carbonate, therefore, increases at depth. The increase in dissolved carbonate occurs faster than any further increase in solubility, causing the carbonate to accumulate within a horizon (Fig. 6), a result that is uncommon for NOPLANT. In simulations of a water-limited environment, where precipitation is entirely consumed through evapotranspiration, the increased dissolved Ca^{2+} accumulates slightly lower in the profile, but in much greater quantities. Where water is less limited, carbonate zoning is still observed, and total carbonate precipitated is still higher in PLANT than NOPLANT, but some dissolved carbonate may escape the system for both (Fig. 6). If plant-affected evapotranspiration is included, which

is typically greater in climates where water is more abundant, the lowering of the carbonate horizon is largely nullified. In NOPLANT, peak carbonate precipitation is often highest in the shallow profile (Fig. 6), and total carbonate is significantly lower. Whether or not the very top layer accumulates dust is controlled by the amount of carbonate dust allowed to build up on the surface.

As described in the methods, the balance between the water holding capacity of the soil and the infiltration of rainwater greatly influences the total accumulation of carbonate possible, as well as its distribution, but the effects of vegetation described above still apply. Simulations were run which lowered the water holding capacity by changing the soil morphology to reflect the young, lapilli ash soils observed at some high latitude sites (Table 1). This greatly increased the depth of carbonate precipitation for both PLANT and NOPLANT simulations. Simulations designed to model the young Yungay profile show that calcite is unlikely to accumulate at depths shallower than 50cm, despite plant cover; this mirrors what was observed in the actual profiles (Table 2). When this lowered field capacity was applied to NOPLANT, carbonate was more likely to accumulate within the 0-50cm range, but in trace amounts. For PLANT, the carbonate horizon still exists, but is found deeper in the profile, and with much higher total carbonate than what is able to precipitate within the NOPLANT case.

DISCUSSION

The Role of Plants in Carbonate Formation

Previous research suggests that the influences of plants on carbonate are myriad, although the explicit link between plants and carbonate formation in the deeper geologic record is quite

recent (Brasier et al., 2011). The effect of plants can be described by their effects on their relevant weathering equations:

silicate weathering:

$CaSiO_3$ (s) + $3H_2O$ +$2CO_2$ (g) = Ca^{2+}(aq) + $2HCO_3^-$(aq) + H_4SiO_4 (aq)

and carbonate weathering:

$CaCO_3$ (s) + H_2O (aq) + CO_2 (g) = Ca^{2+}(aq) + $2HCO_3^-$(aq)

Both reactions are driven to the right by increases in water and CO_2. As soils dewater, the reactions are partially reversed to the point of $CaCO_3$ saturation, and $CaCO_3$ precipitates.

Plants affect these reactions, and subsequently soil carbonate formation, in a variety of ways. Plant respiration directly increases pCO_2 within the soil, and plants improve water retention within soils, both of which drive weathering reactions within the rocks. At the same time plant roots play a large role in physically weathering silicate parent material, increasing the chemically weatherable surface area, as well as increasing the water holding capacity of the soils. Plants also have an effect on dewatering the soils, increasing overall evapotranspiration, lowering surface evapotranspiration, but spreading out the greater total evapotranspiration at depth. The combination of increased weathering and dewatering effectively increases soluble carbonate while also increasing carbonate precipitation rates within the soil profile. Desert plants take up and evapotranspire most infiltrating water in desert soil profiles (e.g. Phillips, 1994; Scanlon et al., 2005), ensuring that the weathering products that plants help to produce are precipitated in the upper few meters of desert soils, and this is often visible as carbonate cementation. In general, the drier the climate the more complete the uptake of soil water by plants. For example, in naturally vegetated plots in southern Nevada ((Gee et al., 1994); MAP

10cm/yr) plants intercepted virtually all rainfall, whereas unvegetated soils experienced little water loss at soil depths >50 cm (Fig. 3).

Our results from the Atacama—including spatial patterns, isotopic composition, and modeling—all link soil carbonate in some way to plants. The more general view (e.g. Jenny and Leonard, 1934; McFadden and Tinsley, 1985) has been that the level of carbonate accumulation is controlled by rainfall and the subsequent degree of leeching, but in the Atacama there is little carbonate accumulation in the absolute desert or the much wetter high Andes, and soil carbonate is most abundant where vegetation is present.

Spatial patterns of soil carbonate within the Atacama clearly implicate the role of plants in their formation. Carbonate of Stage II or greater occurs almost exclusively in the lomas shrubland along the coast and on the flank of the Andes in the Tolar zone between 3300-4200 masl (Fig 5; Table 1). Carbonate diminishes along the margins of these zones where vegetation is sparse, and the soil profiles taken from these transitional zones exhibit reduced carbonate, usually in Stage I or II. In the plantless absolute desert soil profiles show 0-2% carbonate, although it is not visible to the naked eye (Fig 5; Table 1). Above the Tolar zone, crossing over the 0° isotherm, where vegetation fades despite comparatively high precipitation, carbonate is undetectable (Fig 5).

Stable isotopic evidence also provides useful insights into the origin of soil carbonate in the Atacama Desert (e.g. Quade et al., 2007; Rech et al., 2003; Bao et al., 2004). Near the coast, strontium isotopic evidence shows that Ca^{2+} in soil salts derives from marine sources, whereas further inland it comes from reworking of salts that accumulate from ground-water discharge on the many saltpans in the Atacama Desert, likely in the form of eolian gypsum or calcite (Fig. 3E). Fine grained carbonate is present in most but not all saltpans in the Atacama, reaching up to

17% (Quade et al., 2007; Fig. 3 D, E). Previous work has found that the majority of desert soil carbonate formed with calcium sourced from carbonate dust rather than silicate weathering (Gile et al., 1966), a scenario amplified in such a water-limited case as the Atacama Desert.

Carbonate from the absolute desert exhibit $\delta^{13}C$ (PDB) values >+2‰ (Fig. 2, 4), which is consistent with inorganic formation in isotopic equilibrium with ambient atmospheric CO_2. Those samples collected from vegetated areas are mostly <0‰ (Fig. 2, 4), showing an influence of CO_2 derived from C_3 plants; C_4 and CAM (Crassulacean Acid Metabolism) plants are uncommon in the region (Quade et al., 2007). A decrease in isotopic value at depth, observed in the Tolar zone (Fig. 2) and in the transitional zone (Fig. 4) is characteristic of exponentially increasing pCO_2, expected from the increasing contribution of plant respiration.

Few other deserts in the world approach the hyperaridity of the Atacama Desert, where soil chemistry from the dry/cold limit of plants can be compared further. Plantless soils in the southern Negev Desert with rainfall <0.8cm/yr are free of soil carbonate, except for traces of carbonate dust, as in the case of hyperarid soils in the Atacama (Amit et al., 2006). In the even drier Namib Desert, soil carbonate is present up to 17%, but so is evidence of periodic grass cover at the soil sites (Amit et al, 2010), nourished by short and intense rainfall events not experienced in the more equable Negev. The McMurdo Dry Valleys in Antarctica may be the only other modern setting comparable in hyperaridity to the Atacama. As in the driest parts of the Atacama and Negev, soils salts are overwhelmingly gypsic-salic-nitrate, with only trace amounts of carbonate reported, in all but a few cases <3% (Bockheim, 1982, 2002). The McMurdo Dry Valleys exceed both the dry (MAP<1cm/yr) and cold (MAT <<0°C) limit of most plants.

The first order effects of vegetation on carbonate formation are well demonstrated by our carbonate formation model. Plant respiration can increase pCO_2 at shallow depths by orders of magnitude even using the relatively low respiration rates of desert plants (Marion, 1985; Quade, 2007). In those simulations where increasing pCO_2 is the only plant related effect included, the presence of the increasing pCO_2 gradient still significantly increases carbonate precipitation. In water-limited simulations where virtually all infiltrating precipitation is lost to evaporation, all dissolved solute still precipitates out at relatively shallow depths. Where monthly infiltration exceeds monthly evapotranspiration, a carbonate "trap" is created, induced by an ever enlarging supply of dissolved carbonate. When the plant effects on total evapotranspiration and its distribution are included, they serve to decrease the depth at which the carbonate horizon precipitates, but do not drastically alter the vertical profile distribution.

Beyond these first-order effects, both the laboratory measurements and manipulation of soil morphologies within the simulation show that the most overwhelming influence on carbonate formation provided by plants might be the long term weathering effect on the evolution of soils. The field capacity term was very important, both in terms of the total carbonate generated, and in the distribution of carbonate when realistic morphologic variations with depth are included. The general break down of silicate material within the soil is a large component of this, but the accumulation of organic matter also has a noticable effect on available water content. The ability of active root systems to create an environment where organics can concentrate greatly increases soil capacity and subsequently the amount of carbonate that can precipitate.

Additional simulations were performed to compare the concentrated precipitation events, like what is seen in the Namib, to the more equable rain patterns seen in Negev. These tests show

that the highly concentrated annual precipitation events transport similar amounts of carbonate to the more equable precipitation distributions, but carry solutes much deeper within the profile. This actually creates less accumulation of soil carbonate than a more moderate rainfall distribution, as some of the material can potentially be lost from the vadose zone. The only way to reproduce the very high carbonate abundances, akin to what is seen in the Namib Desert, is to add the effect of plants which both increases the overall amount of carbonate and creates a transpiration induced trap, effectively concentrating carbonate into a K-horizon.

Additional Influences on Soil Salt Formation

The Atacama Desert's unique climate transitions allow us to observe additional influences on soil salt formation. The high concentration of soluble sulfate, nitrate, and chloride within the absolute desert is found in few other parts of the world. Soluble salt profiles tend to fit one of two distributions: either an approximately equable distribution or one where abundances strongly increase with depth (Table 2). The frequency of rainfall (Fig. 2, Table 1) appears to be the main determinant in carrying the soluble salts farther down in the profile. Sites with a more even distribution, and consequently less record of infiltration, appear also to concentrate carbonate in shallower zones, an anticipated outcome from less frequent or heavy precipitation events. Were the distribution of these salts entirely controlled by respective solubilities sulfate should decrease less in the zones with higher precipitation than nitrate or chloride. That sulfate decreases the most is possibly a result of chloride and nitrate fixation in zones with plant cover (Phillips, 1994; Scanlon et al., 2005; Walvoord et al., 2003).

Carbonate is highest in those zones where the more soluble salts are lowest. The inverse relationship between carbonate and sulfate within the same layers is the most extreme example of this, where the presence of SO_4 in solution greatly increases the solubility of carbonate, and

can inhibit crystallization (Chong and Sheikholeslami, 2001). This effect on carbonate solubility potentially enhances the shallow concentrations of carbonate in the absolute desert where sulfate shows the largest gradient, and is highest in the lower part of the profile. One of the few layers where both high sulfate and carbonate are observed is the 40-50cm layer of YUN2029 which sits directly above cemented gypcrete. A barrier to flow related to the gypcrete could explain the high levels of carbonate and its correspondence with sulfate, effectively trapping and precipitating carbonate where dissolved carbonate is highest.

Visible dust transport can be observed even at high elevations, but in the younger soils carbonate is virtually non-existent. Here, precipitation limits rather than promotes the accumulation of carbonate on the soil surface. Salt dust is kept from accumulating at these high elevations, either by reworking or dissolution and transport to the deeper subsurface. The same phenomenon can be seen in the other salts where abundances are at their lowest levels. More evolved soil morphologies with higher water capacities would shallow the depth of carbonate precipitation, and produce higher volumes of soil carbonate, similar to those recorded in other parts of the Tolar zone, though precipitation would still limit the concentration of the more soluble salts.

Implications for Martian Soils

In general, secondary salts in soils on Mars display a very Atacama-like pattern. Like Mars, the soils in the Atacama are dominated by sulfates and chlorides, and also like Martian soils Atacama soils from the absolute desert profiles have an unusually high S/Cl ratio compared to most terrestrial soils (Clark and Hart, 1981), or to those profiles where vegetation and precipitation are higher. The Atacama is one of the few locations on Earth where perchlorates can be considered a portion of the chlorine budget, and their formation has been studied as a

Martian analog (Catling et al., 2010). Finally, carbonate in soils from both the hyperarid desert and Mars appears generally limited to <5% and the portion that persists is likely eolian in origin.

The distribution of carbonate discovered on Mars to date fits well in the framework of our Atacama observations, and the similarities between the Atacama and Mars offer insight into why carbonate is so scarce on the modern Martian surface. Without plant cover, and with a porous, underdeveloped regolith, bicarbonate would have percolated deep into the water table and either precipitated at depth in the subsurface, or have been involved in alteration reactions. The few substantial deposits that are seen on the surface of Mars likely fall into one of these eventualities. Numerous meteorites identified as Martian in origin contain carbonate in low amounts (<1%), often as part of younger alteration assemblages (Bridges et al., 2001). ALH84001, which has the most abundant carbonate of the Martian meteorites, has a composition indicative of low temperature diagenetic alteration in the shallow subsurface (Romanek et al., 1994). The first remotely detected outcrop-scale carbonate has been interpreted as magnesite which was likely altered from adjacent olivine, potentially by percolating groundwater (Ehlmann et al., 2008). While prior rover missions failed to detect carbonate outcrops on the surface, the Spirit rover detected an olivine-carbonate assemblage, with 18-36% magnesium- and iron-rich carbonate that is interpreted as a hydrothermal alteration of Noachian material (Morris et al., 2010). In two deeply exhumed Noachian craters, carbonate has been discovered which is potentially related to groundwater interactions (Michalski and Niles, 2010; Michalski et al., 2013). Carbonate/smectite/olivine assemblages also have recently been identified in the Libya Montes region, again likely related to hydrothermal alteration (Bishop, 2013). Although hyperspectral coverage of Mars's surface is widespread, and the search for carbonate continues,

these are the only firm carbonate identifications to date, and none of them definitively formed on the surface.

Martian fines have been relatively homogenous between globally separate landing sites, indicating eolian processes as the primary dispersal agent for the past few billion years. A poorly evolved soil and a lack of vegetation would have resulted in reduced weathering rates, and weathering products would be more likely to escape the vadose zone. Those trace quantities of carbonate in dust and soils were likely produced from either very reduced weathering of silicates or possibly recycling from exposed alteration suites or salt-pan particulates, perhaps from more easily weathered, carbonate-like versions of the apparent chloride salt-pan deposits (Osterloo et al., 2008), comparable to the Atacama salars. Regardless of surface condition changes which might have occurred on Mars, even erasing what early carbonate record did exist (Fairen et al., 2004), the majority of carbonate on Mars would have been transported deep into the groundwater table, and would have resulted in precipitation or alteration at depth. Indeed, this model of carbonate formation fits within the more recent characterization of carbonate formation on Mars that assigns the majority of pH-neutral salt formation to the subsurface (Ehlmann, et al., 2011), and which implies a potentially vast reservoir of carbonate and other alteration minerals in the subsurface (e.g. Michalski et al., 2010; Niles et al., 2012)

The absence of plant-induced effects that were relevant for Atacama soils would also be relevant for Mars, and can be demonstrated within our model. Raising the overall pCO_2 without creating a gradient with depth increases the total amount of dissolved carbonate and lowers the depth at which accumulation occurs but does not induce the formation of a carbonate horizon, as in the case of an exponential CO_2 increase. Lowering the field capacity to reflect a Mars-like brecciated surface would similarly lower the depth of precipitation, and an early Mars would

have the additional effect of a reduced surface energy flux, effectively lowering evaporation, and again the depth of precipitation. While not formally considered in our model, a Mg^{2+}-dominated water chemistry, similar to what likely formed the carbonate in ALH84001, would again increase the solubility of carbonate, as magnesite has a solubility several times higher than calcite or aragonite, dependent on pCO_2 and temperature.

CONCLUSION

The Atacama Desert offers the unique opportunity to investigate how soil carbonate is distributed across a range of climates with variable plant cover. Consistently, those regions with plants have more well developed carbonate horizons than those regions without vegetation, and much higher carbonate fractions. In contrast to this, soils in the absolute desert contain only trace (<3%) carbonate and in the high Andes, where precipitation is substantially higher but conditions are too cold for plants, no carbonate is present. The influence of plants on carbonate formation can also be detected isotopically. The traces of carbonate found in the plantless absolute desert generally have $\delta^{13}C$ values >+2‰, and formed in equilibrium with the atmosphere. Values in vegetated areas are <0‰ due to the influence of plant CO_2.

Plants cause an increase in total evapotranspiration, and in pCO_2 and dewatering with soil depth. Our carbonate precipitation model demonstrates that the presence of plants across virtually all soil morphologies increases the total budget of dissolved carbonate. Plants also focus carbonate formation into a narrow depth range and reduce the maximum depth of precipitation. Although the long-term effects of silicate weathering were not included in our model, the importance of soil evolution to trapping infiltrating precipitation is demonstrated in both the soil transects and within the simulations. The increase in silicate weathering provided by

plants would have a large effect on soil morphology, and therefore in decreasing the depth of carbonate precipitation. The absence of plants on Mars or on the early Earth should have resulted in reduced soil carbonate production, with the majority of dissolved solutes simply percolating to depth, either to be transported to larger reservoirs or precipitated deep within the subsurface.

REFERENCES

Amit, R., Enzel, Y., Grodek, T., Crouvi, O., Porat, N., and Ayalon, A., 2010, The role of rare rainstorms in the formation of calcic soil horizons on alluvial surfaces in extreme deserts: Quaternary Research, v. 74, no. 2, p. 177-187.

Amit, R., Enzel, Y., and Sharon, D., 2006, Permanent Quaternary hyperaridity in the Negev, Israel, resulting from regional tectonics blocking Mediterranean frontal systems: Geology, v. 34, no. 6, p. 509-512.

Arroyo, M. T. K., Squeo, F. A., Armesto, J. J., and Villagran, C., 1988, Effects of aridity on plant diversity in the northern Chilean Andes: results of a natural experiment: Annals of the Missouri Botanical Garden, p. 55-78.

Asner, G. P., Scurlock, J. M., and A Hicke, J., 2003, Global synthesis of leaf area index observations: implications for ecological and remote sensing studies: Global Ecology and Biogeography, v. 12, no. 3, p. 191-205.

Bao, H., Jenkins, K. A., Khachaturyan, M., and Díaz, G. C., 2004, Different sulfate sources and their post-depositional migration in Atacama soils: Earth and Planetary Science Letters, v. 224, no. 3, p. 577-587.

Bishop, J. L., Perry, K. A., Darby Dyar, M., Bristow, T. F., Blake, D. F., Brown, A. J., and Peel, S. E., 2013, Coordinated spectral and XRD analyses of magnesite-nontronite-forsterite mixtures and implications for carbonates on Mars: Journal of Geophysical Research: Planets, v. 118, no. 4, p. 635-650.

Blaney, D. L., and McCord, T. B., 1989, An observational search for carbonates on Mars: Journal of Geophysical Research: Solid Earth (1978–2012), v. 94, no. B8, p. 10159-10166.

Bockheim, J., 1982, Properties of a chronosequence of ultraxerous soils in the Trans-Antarctic Mountains: Geoderma, v. 28, no. 3, p. 239-255.

Bockheim, J., 2002, Landform and soil development in the McMurdo Dry Valleys, Antarctica: a regional synthesis: Arctic, Antarctic, and Alpine Research, p. 308-317.

Boynton, W., Ming, D., Kounaves, S., Young, S., Arvidson, R., Hecht, M., Hoffman, J., Niles, P., Hamara, D., and Quinn, R., 2009, Evidence for calcium carbonate at the Mars Phoenix landing site: Science, v. 325, no. 5936, p. 61-64.

Bridges, J. C., Catling, D., Saxton, J., Swindle, T., Lyon, I., and Grady, M., 2001, Alteration assemblages in Martian meteorites: Implications for near-surface processes, Chronology and evolution of Mars, Springer, p. 365-392.

Calvin, W. M., King, T. V., and Clark, R. N., 1994, Hydrous carbonates on Mars?: Evidence from Mariner 6/7 infrared spectrometer and ground-based telescopic spectra: Journal of Geophysical Research: Planets (1991–2012), v. 99, no. E7, p. 14659-14675.

Carr, M. H., 1996, Water on Mars: New York: Oxford University Press,| c1996, v. 1.

Catling, D., Claire, M., Zahnle, K., Quinn, R., Clark, B., Hecht, M., and Kounaves, S., 2010, Atmospheric origins of perchlorate on Mars and in the Atacama: Journal of Geophysical Research: Planets (1991–2012), v. 115, no. E1.

Cazemier, D., Lagacherie, P., and Martin-Clouaire, R., 2001, A possibility theory approach for estimating available water capacity from imprecise information contained in soil databases: Geoderma, v. 103, no. 1, p. 113-132.

Chong, T., and Sheikholeslami, R., 2001, Thermodynamics and kinetics for mixed calcium carbonate and calcium sulfate precipitation: Chemical engineering science, v. 56, no. 18, p. 5391-5400.

Christensen, P., Wyatt, M., Glotch, T., Rogers, A., Anwar, S., Arvidson, R., Bandfield, J., Blaney, D., Budney, C., and Calvin, W., 2004, Mineralogy at Meridiani Planum from the Mini-TES experiment on the Opportunity Rover: Science, v. 306, no. 5702, p. 1733-1739.

Clark, B. C., and Van Hart, D. C., 1981, The salts of Mars: Icarus, v. 45, no. 2, p. 370-378.

Cousin, I., Nicoullaud, B., and Coutadeur, C., 2003, Influence of rock fragments on the water retention and water percolation in a calcareous soil: Catena, v. 53, no. 2, p. 97-114.

Drees, K. P., Neilson, J. W., Betancourt, J. L., Quade, J., Henderson, D. A., Pryor, B. M., and

Maier, R. M., 2006, Bacterial community structure in the hyperarid core of the Atacama Desert, Chile: Applied and environmental microbiology, v. 72, no. 12, p. 7902-7908.

Ehlmann, B. L., Mustard, J. F., Murchie, S. L., Bibring, J.-P., Meunier, A., Fraeman, A. A., and Langevin, Y., 2011, Subsurface water and clay mineral formation during the early history of Mars: Nature, v. 479, no. 7371, p. 53-60.

Ehlmann, B. L., Mustard, J. F., Murchie, S. L., Poulet, F., Bishop, J. L., Brown, A. J., Calvin, W. M., Clark, R. N., Des Marais, D. J., and Milliken, R. E., 2008, Orbital identification of carbonate-bearing rocks on Mars: Science, v. 322, no. 5909, p. 1828-1832.

Fairén, A. G., Fernández-Remolar, D., Dohm, J. M., Baker, V. R., and Amils, R., 2004, Inhibition of carbonate synthesis in acidic oceans on early Mars: Nature, v. 431, no. 7007, p. 423-426.

Gee, G., Wierenga, P., Andraski, B., Young, M., Fayer, M., and Rockhold, M., 1994, Variations in water balance and recharge potential at three western desert sites: Soil Science Society of America Journal, v. 58, no. 1, p. 63-72.

Gile, L. H., Peterson, F. F., and Grossman, R. B., 1966, Morphological and genetic sequences of carbonate accumulation in desert soils: Soil Science, v. 101, no. 5, p. 347-360.

Hirmas, D. R., Amrhein, C., and Graham, R. C., 2010, Spatial and process-based modeling of soil inorganic carbon storage in an arid piedmont: Geoderma, v. 154, no. 3, p. 486-494.

Houston, J., 2006, Variability of precipitation in the Atacama Desert: its causes and hydrological impact: International Journal of Climatology, v. 26, no. 15, p. 2181-2198.

Jenny, H., and Leonard C. D., 1934, Functional relationships between soil properties and rainfall: Science, v. 38, no. 5, p. 363-382.

Kraimer, R. A., and Monger, H. C., 2009, Carbon isotopic subsets of soil carbonate—A particle comparison of limestone and igneous parent materials: Geoderma, v. 150, no. 1, p. 1-9.

Latorre, C., Betancourt, J. L., Rylander, K. A., and Quade, J., 2002, Vegetation invasions into absolute desert: A 45; th000 yr rodent midden record from the Calama–Salar de Atacama basins, northern Chile (lat 22°–24° S): Geological Society of America Bulletin, v. 114, no. 3, p. 349-366.

Latorre, C., Betancourt, J. L., Rylander, K. A., and Quade, J., 2002, Vegetation invasions into

absolute desert: A 45; th000 yr rodent midden record from the Calama–Salar de Atacama basins, northern Chile (lat 22°–24° S): Geological Society of America Bulletin, v. 114, no. 3, p. 349-366.

Leshin, L., Mahaffy, P., Webster, C., Cabane, M., Coll, P., Conrad, P., Archer, P., Atreya, S., Brunner, A., and Buch, A., 2013, Volatile, isotope, and organic analysis of martian fines with the Mars Curiosity rover: Science, v. 341, no. 6153, p. 1238937.

Marion, G. M., Schlesinger, W., and Fonteyn, P., 1985, CALDEP: A regional model for soil CaCO3 (caliche) deposition in southwestern deserts: Soil Science, v. 139, no. 5, p. 468.

Marshall, W. L., and Slusher, R., 1968, Aqueous systems at high temperature. Solubility to 200. degree. of calcium sulfate and its hydrates in sea water and saline water concentrates, and temperature-concentration limits: Journal of Chemical & Engineering Data, v. 13, no. 1, p. 83-93.

Mayer, L., 1986, The distribution of calcium carbonate in soils: A computer simulation using program CALSOIL, US Department of the Interior, Geological Survey.

Mayer, L., McFadden, L. D., and Harden, J. W., 1988, Distribution of calcium carbonate in desert soils: A model: Geology, v. 16, no. 4, p. 303-306.

McAuliffe, J. R., 1990, A rapid survey method for the estimation of density and cover in desert plant communities: Journal of Vegetation Science, v. 1, no. 5, p. 653-656.

Meyer, N. A., Breecker, D. O., Young, M. H., and Litvak, M. E., 2014, Simulating the Effect of Vegetation in Formation of Pedogenic Carbonate: Soil Science Society of America Journal, v. 78, no. 3, p. 914-924.

McFadden L. D. and Tinsley J. C., 1985, Rate and depth of pedogenic carbonate accumulation in soils: Formulation and testing of a compartment model: Geological Society of America Special Papers, v. 203, p. 23-42.

Michalski, G., Böhlke, J., and Thiemens, M., 2004, Long term atmospheric deposition as the source of nitrate and other salts in the Atacama Desert, Chile: New evidence from mass-independent oxygen isotopic compositions: Geochimica et Cosmochimica Acta, v. 68, no. 20, p. 4023-4038.

Michalski, J. R., Cuadros, J., Niles, P. B., Parnell, J., Rogers, A. D., and Wright, S. P., 2013, Groundwater activity on Mars and implications for a deep biosphere: Nature Geoscience, v. 6, no. 2, p. 133-138.

Michalski, J. R., and Niles, P. B., 2010, Deep crustal carbonate rocks exposed by meteor impact on Mars: Nature Geoscience, v. 3, no. 11, p. 751-755.

Monger, H. C., Cole, D. R., Buck, B. J., and Gallegos, R. A., 2009, Scale and the isotopic record of C4 plants in pedogenic carbonate: from the biome to the rhizosphere: Ecology, v. 90, no. 6, p. 1498-1511.

Morris, R. V., Ruff, S. W., Gellert, R., Ming, D. W., Arvidson, R. E., Clark, B. C., Golden, D., Siebach, K., Klingelhöfer, G., and Schröder, C., 2010, Identification of carbonate-rich outcrops on Mars by the Spirit rover: Science, v. 329, no. 5990, p. 421-424.

Navarro-González, R., Rainey, F. A., Molina, P., Bagaley, D. R., Hollen, B. J., de la Rosa, J., Small, A. M., Quinn, R. C., Grunthaner, F. J., and Cáceres, L., 2003, Mars-like soils in the Atacama Desert, Chile, and the dry limit of microbial life: Science, v. 302, no. 5647, p. 1018-1021.

Neitsch, S., Arnold, J., Kiniry, J., and Williams, J., 2005, Soil and water assessment tool (SWAT), theoretical documentation. Blackland Research Center, Grassland: Soil and Water Research Laboratory, Agricultural Research Service, Temple, TX.

Niles, P. B., Catling, D. C., Berger G., Chassefiere, E., Ehlmann, B. L., Michalski, J. R., Morris, R., Ruff, S. W., and Sutter, B., 2012, 2013, Geochemistry of carbonates on Mars: Implications for climate history and nature of aqueous environments: Space Science Reviews, v. 174, p. 301-328.

Osterloo, M., Hamilton, V., Bandfield, J., Glotch, T., Baldridge, A., Christensen, P., Tornabene, L., and Anderson, F., 2008, Chloride-bearing materials in the southern highlands of Mars: Science, v. 319, no. 5870, p. 1651-1654.

Phillips, F. M., 1994, Environmental tracers for water movement in desert soils of the American Southwest: Soil Science Society of America Journal, v. 58, no. 1, p. 15-24.

Pollack, J. B., Kasting, J. F., Richardson, S. M., and Poliakoff, K., 1987, The case for a wet, warm climate on early Mars: Icarus, v. 71, no. 2, p. 203-224.

Prellwitz, J., 2007, A characterization of hyper-arid nitrate soils in the Baquedano Valley of the Atacama Desert, northern Chile [MS thesis], Oxford, Ohio, Miami University.

Quade, J.,. Cerling T. E, and Bowman J. R., 1990, Stable isotopes from desert soil carbonates in paleoecologic reconstruction. Seventh international conference on geochronology, cosmochronology and isotope geology.

Quade, J., Rech, J. A., Latorre, C., Betancourt, J. L., Gleeson, E., and Kalin, M. T., 2007, Soils at the hyperarid margin: The isotopic composition of soil carbonate from the Atacama Desert, Northern Chile: Geochimica et Cosmochimica Acta, v. 71, no. 15, p. 3772-3795.

Rawls, W., Brakensiek, D., and Saxton, K., 1982, Estimation of soil water properties: Trans. Asae, v. 25, no. 5, p. 1316-1320.

Rech, J. A., Quade, J., and Hart, W. S., 2003, Isotopic evidence for the source of Ca and S in soil gypsum, anhydrite and calcite in the Atacama Desert, Chile: Geochimica et Cosmochimica Acta, v. 67, no. 4, p. 575-586.

Romanek, C. S., Grady, M. M., Wright, I., Mittlefehldt, D., Socki, R., Pillinger, C., and Gibson, E., 1994, Record of fluid rock interactions on Mars from the meteorite ALH84001: Nature, v. 372, no. 6507, p. 655-657.

Rundel, P. W., Dillon, M. O., Palma, B., Mooney, H., Gulmon, S., and Ehleringer, J., 1991, The phytogeography and ecology of the coastal Atacama and Peruvian deserts: Aliso, v. 13, no. 1, p. 1-49.

Scanlon, B., Levitt, D., Reedy, R., Keese, K., and Sully, M., 2005, Ecological controls on water-cycle response to climate variability in deserts: Proceedings of the National academy of Sciences, v. 102, no. 17, p. 6033-6038.

Smith, P., Tamppari, L., Arvidson, R., Bass, D., Blaney, D., Boynton, W., Carswell, A., Catling, D., Clark, B., and Duck, T., 2009, H2O at the Phoenix landing site: Science, v. 325, no. 5936, p. 58-61.

Thornthwaite, C. W., 1948, An approach toward a rational classification of climate: Geographical review, p. 55-94.

Toulmin, P., Baird, A., Clark, B., Keil, K., Rose, H., Christian, R., Evans, P., and Kelliher, W., 1977, Geochemical and mineralogical interpretation of the Viking inorganic chemical results: Journal of Geophysical Research, v. 82, no. 28, p. 4625-4634.

Valdivia-Silva, J. E., Navarro-González, R., Fletcher, L., Perez-Montaño, S., Condori-Apaza, R., and Mckay, C. P., 2012, Soil carbon distribution and site characteristics in hyper-arid soils of the Atacama Desert: a site with Mars-like soils: Advances in Space Research, v. 50, no. 1, p. 108-122.

Villagrán, C., Armesto, J., and Arroyo, M. K., 1981, Vegetation in a high Andean transect between Turi and Cerro León in northern Chile: Vegetatio, v. 48, no. 1, p. 3-16.

Villagrán, C., Kalin, M., and Marticorena, C., 1983, Efectos de la desertizacion en la distribucién de la flora andina de Chile: Revista Chilena de Historia Natural, v. 56, p. 137-157.

Walvoord, M. A., Phillips, F. M., Stonestrom, D. A., Evans, R. D., Hartsough, P. C., Newman, B. D., and Striegl, R. G., 2003, A reservoir of nitrate beneath desert soils: Science, v. 302, no. 5647, p. 1021-1024.

FIGURES AND FIGURE CAPTIONS

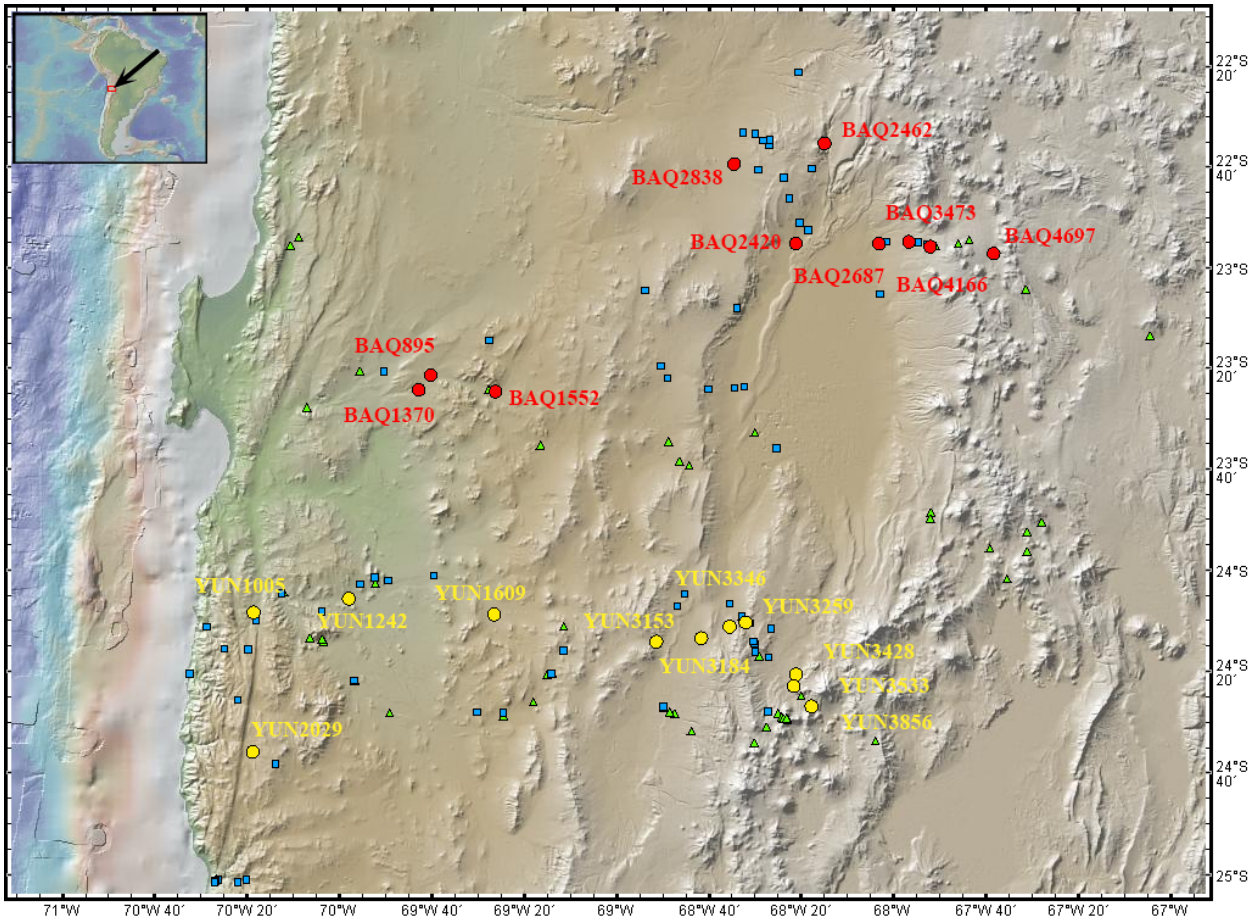

Figure 1. Study area of Chilean sites used in this study. Full location data can be found in Table 1. Green triangles are observations of carbonate cementations. Blue squares include both carbonate observations as well as isotopic analysis. Red and yellow circles are the Baquedano and Yungay soil pit transects.

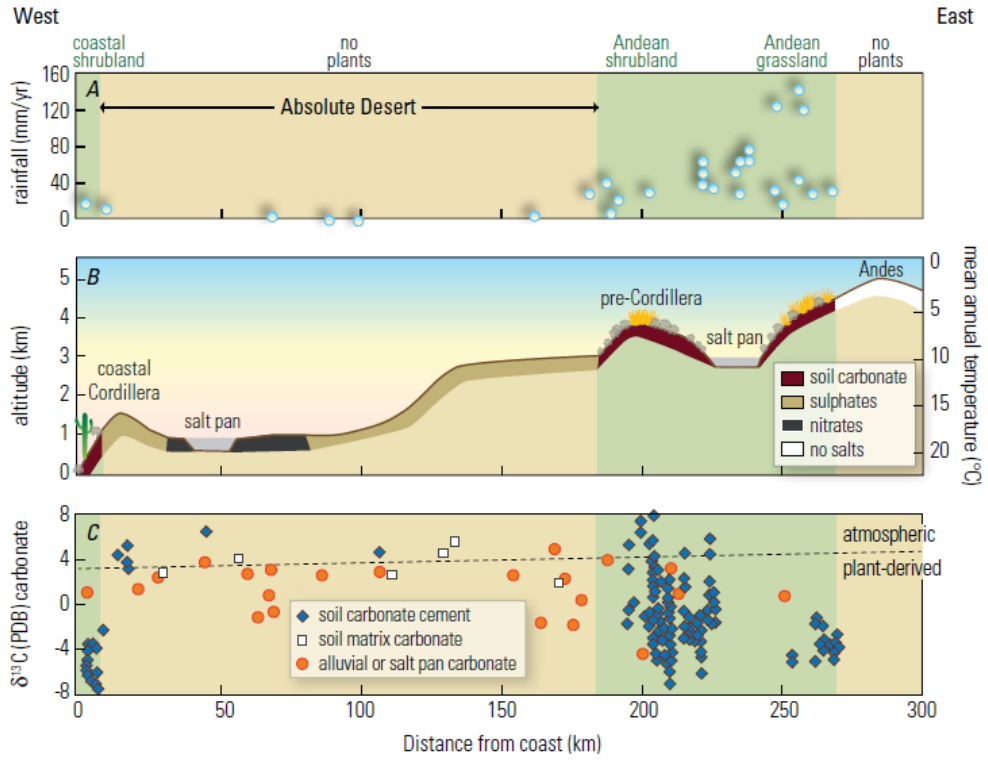

Figure 2. Observations along an east-west transect across the Atacama Desert at 22-24°S. a) mean annual rainfall. b) generalized topographic profile showing the distribution of the important soil salts. c) the $\delta^{13}C$ value (PDB) of carbonate in modern soils as cements, as matrix in soils in the Absolute Desert, and in alluvial and saltpan silt. The sub-horizontal dashed line denotes the predicted $\delta^{13}C$ value of carbonate formed in equilibrium with atmospheric CO_2, which varies slightly with temperature. Carbonate influenced by plant-derived CO_2 would fall below this line.

Figure 3. Photographs of study sites in northern Chile: (A) soil site BAQ-895, absolute desert, (B) soil site BAQ-4166, *Stipa-Festuca* grassland, (C) soil site Paposo-120, coastal lomas vegetation, with whitish calcic horizon (Bk) indicated, (D) soil site SOC 3305 m (AD04-46), with reddish (5YR 6/4dry) clay-rich (Bt) and whitish calcic horizon (s) (Bk) indicated, (E) stromatolitic heads in salar brine, and surrounding marly muds (indicated), southern Salar de Atacama, 2302 masl and (F), white marls in foreground and airborne marl in background, Salar de Pujsa, 4521 masl.

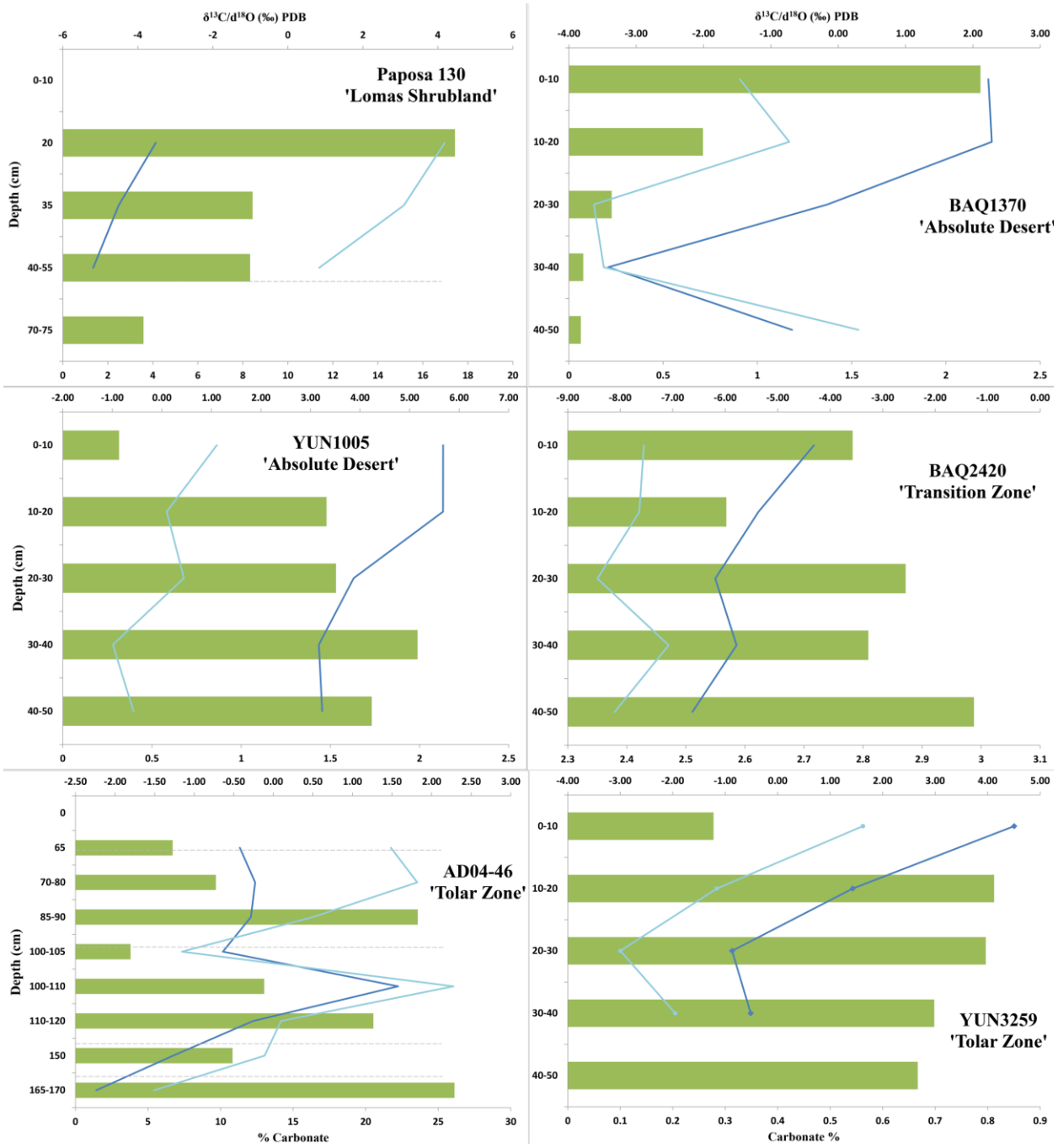

Figure 4. Panel of six representative soil pit profiles; for full data see Table 2. Vertical axis is depth in cm. The top horizontal axis is $\delta^{13}C$ and $\delta^{18}O$ (‰) PDB where the dark blue lines are $\delta^{13}C$ and the light blue lines are $\delta^{18}O$. Green bars describe carbonate mass % within the soil. The top left is from the coastal lomas where vegetation is present. The absolute desert profiles have no vegetation. The transition zone had no visible vegetation but did have evidence for temporal vegetation in the soil and there was vegetation in surrounding washes. The tolar zone has variable vegetation.

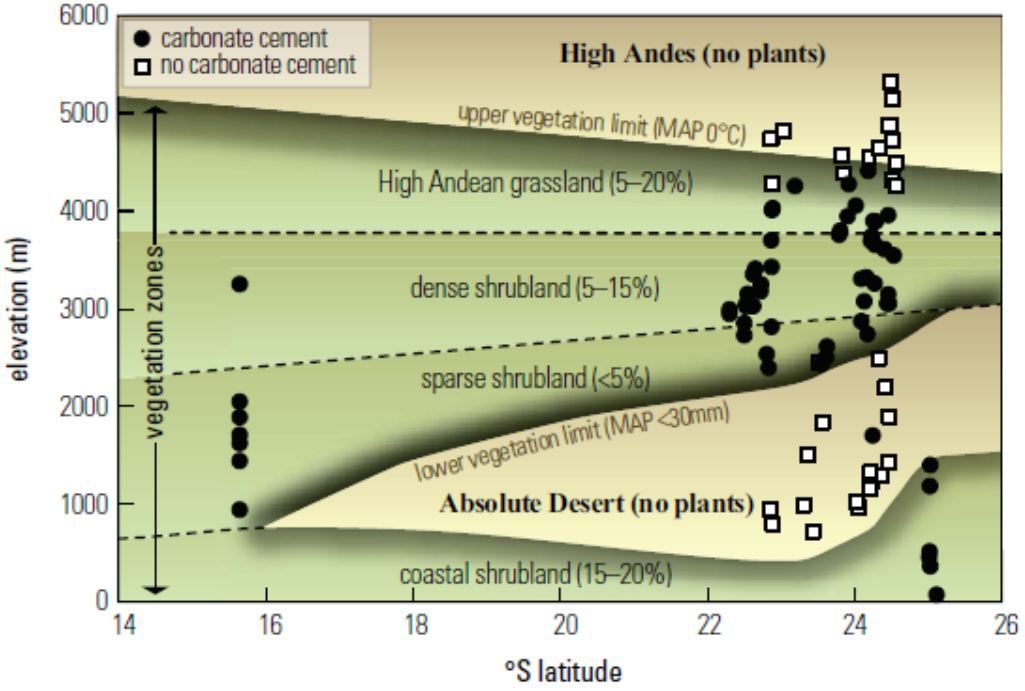

Figure 5. Distribution of soils with and without visible soil carbonate cementation (Stages I-IV; see Table 1 for site data) with latitude and elevation in the Atacama Desert. Vegetated areas are in green, with the main vegetation zones labeled and separated by dashed lines, as well as the range of percent vegetation cover in each zone (Latorre C. et al., 2011).

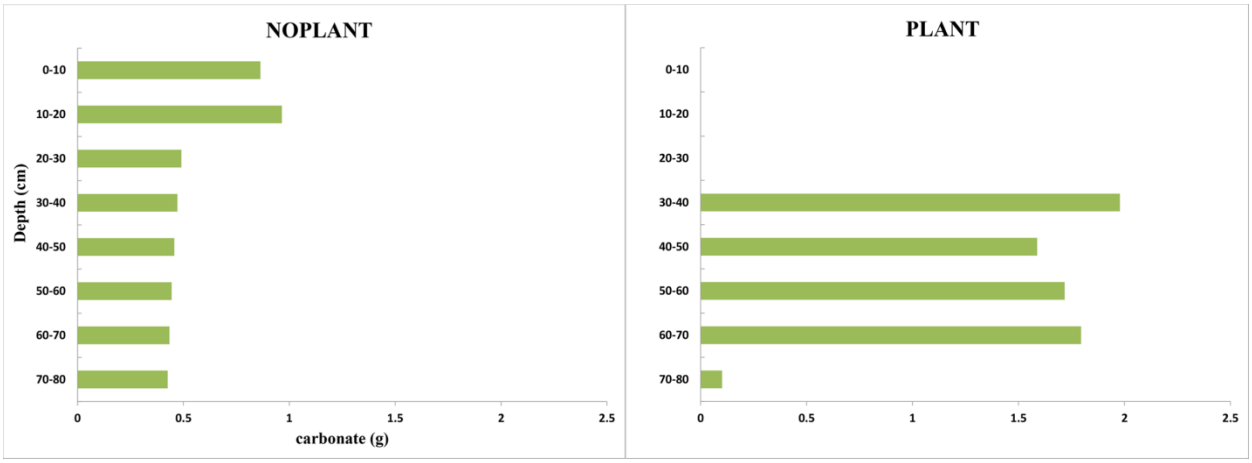

Figure 6. Two characteristic model simulations using the NOPLANT and PLANT parameterizations. Simulations were run over 10^4 yrs, with 15cm/yr annual precipitation, 0.01g initial carbonate at each layer, and with climate and morphologic parameters similar to a high elevation >3500 masl Atacama site. The accumulation at the 0-10cm depth is the result of an accumulation of carbonate dust. The PLANT simulation forms a clear carbonate horizon, effectively trapping all transported carbonate that is leached from the surface. The NOPLANT simulation accumulates carbonate dust at the surface if no removal mechanism is included in the model, and much of the carbonate that is dissolved is lost at the base of the model.

SUPPLEMENT A: FULL MODEL DESCRIPTION

The fundamental design of the model was based on CALSOIL 2.0 (Meyer et al., 1988) and is described within the methods section. The original model requires specific inputs for each compartment. To allow for variations in compartment depth and number of compartments, many of these specific parameters were replaced with regression functions. Specific to the PLANT and NOPLANT experiments adjustments were made to pCO_2 with depth, and evapotranspiration. In the scenario where plant cover was absent, pCO_2 was kept constant with depth. For those simulations concerning the Atacama Desert this was kept at 270ppm, but this was increased to examine the effect of past climates on Mars and Earth. Total evapotranspiration was calculated using the Thornwaithe method (Thornwaithe, 1948), and was one of the original two methods provided by the CALSOIL 2.0 model. While this is not a perfect estimate for Actual Evapotranspiration (AET) it was used over more rigorous models for two reasons: It relies only on temperature and location data, which were both well constrained, and it assumes a certain level of plant cover. Typically the Thornwaithe model can under-predict Potential Evapotranspiration (PET) for hyperarid environments, but because our model did not correct for the decrease in evaporation under unsaturated conditions this effect was desirable. To separate out transpiration from evaporation we used the equation:

$$E_t = \frac{E_T \cdot LAI}{3.0}$$

where E_t is the transpiration component of evapotranspiration, E_T is total PET, and LAI is the leaf area index (Neitsch, et al., 2005). The LAI for most simulations was assumed to be 1.3, which matches typical desert vegetation (Asner et al, 2003), though multiple LAI values were examined. Evaporation was then assumed to be any remaining portion of the total evapotranspiration. To adjust the distribution of potential evapotranspiration with depth two

separate regression functions were made, and integrated to normalize the equations to one. These regression equations were based on evaporation rates observed within the Atacama and transpiration rates predicted for desert vegetation (Meyer, 1998; Marion et al., 1985; Houston, 2006). Normalized regression equations effectively acted like the PETINDEX term in the original CALSOIL 2.0 model. Variations were tested for each of these regression equations but they did not greatly affect the model results so long as transpiration declined less drastically than evaporation. For the NOPLANT case only the evaporation term was applied, and for the PLANT scenario the total original evapotranspiration was applied with a combined regression function normalized to one. Total evapotranspiration was modified as desired by a scalar to match and explore a range of reasonable annual evapotranspiration values for arid and hyperarid deserts.

The original CALSOIL model required a number of individual inputs for each layer, including field capacity, wilting point, compartment temperature and starting carbonate. Field capacity and wilting point were calculating using the Rawls equations (Rawls et al., 1982) which require silt, clay, sand, and organic matter content. Soil morphologies were estimated from existing samples and field descriptions, and organic matter was included in PLANT based on average values measured from our sample sites (to be included in a separate publication.) Because stone content was included, but not a part of the original Rawls equations, all stone content was assumed to be "sand" (the coarsest grain size) for calculating field capacity and wilting point. These numbers were adjusted over a range of values relevant to desert soils (Marion et al., 1985). Soil morphologic contents were generally kept static with depth, but for certain tests were adjusted based on field descriptions of variations observed. Compartment temperature was assumed to be the annual temperature average, and constant with depth. Adjustments had little effect on carbonate solubility compared to total pCO_2.

This model was limited in a number of ways that should also be discussed. Newer models which have tried to calculate carbonate precipitation have used flow models which allow bidirectional flow in unsaturated or saturated zones (Meyer et al., 2014). For surface layers of the Atacama, bi-directional flow is likely unnecessary outside of the salars. Our model is also limited in that it cycles on monthly rather than smaller timescales, essentially summing evaporation and precipitation and acting it out all at once. Though it would be simple to adapt this simulation for smaller timescales, the infrequency of precipitation events makes this unnecessary.

The model lacks any consideration for bacterial respiration, because for hyperarid environments like the absolute desert, or Mars, this can be assumed to be an extremely small contributor compared to the potential increase in pCO_2 from plants.

The model does not budget other salts in conjunction with carbonate. While Cl^- has been shown to have little to no influence on the solubility of calcite (Marshall and Slusher, 1968), SO_4^{-2} drastically increases the solubility of carbonate. Ideally the model should be adapted to balance and transport gypsum at each layer.

SUPPLEMENT B: DATA TABLES

Table 1.

soil site	elevation (m)	latitude (S)[a]	longitude (W)[a]	vegetation cover	MAT[b] °C	MAP[b] mm/yr	estimated age yrs
BAQ895	895	23.40284	69.714	0	16.6	10	$>10^6$
BAQ1370	1370	23.35399	69.67095	0	15.2	23	10^4-10^5
BAQ1552	1552	23.40907	69.43716	0	14.5	30	$>10^6$
BAQ2420	2420	22.91800	68.35321	0	10.0	72	10^3-10^4
BAQ2462	2462	22.58.547	68.24.990	0	9.7	75	10^3-10^4
BAQ2838	2838	22.65381	68.57623	0	7.1	99	10^4-10^5
BAQ2687	2687	22.91826	68.05260	< 1	8.2	89	10^4-10^5
BAQ3473	3473	22.91243	67.94506	1.2	1.8	148	10^3-10^4
BAQ4166	4166	22.92870	67.86801	7.1	-5.1	213	10^3-10^4
BAQ4697	4697	22.95144	67.63925	< 1	-11.3	271	10^3-10^4
YUN2029	2029	24.59522	70.31290	0	12.2	51	$>10^6$
YUN1005	1005	24.09232	69.96649	0	16.3	0.2[d]	$>10^6$
YUN1242	1242	.24.13768	70.31030	0	15.6	0.2[d]	$>10^6$
YUN1609	1609	24.14393	69.44164	0	14.2	32	10^3-10^4
YUN3184	3184	24.22212	68.69446	0	4.4	125	$>10^6$
YUN3153	3153	24.23397	68.85687	0	4.6	122	10^3-10^4
YUN3259	3259	24.17038	68.53411	2.4	3.7	131	10^4-10^5
YUN3346	3346	24.18463	63.59200	<<1	3.0	138	10^5-10^6?
YUN3428	3428	24.34145	68.35245	8.8	2.2	145	10^3-10^4
YUN3533	3533	24.37960	68.36074	8.6	1.3	154	10^3-10^4
YUN3856	3856	24.44625	68.29658	3.1	-1.8	183	10^3-10^4
SOC 3371	3371	24.28820	68.45119	6.6	2.7	140	10^5-10^6
Paposo 130	130	25.10625	70.47324	17.8	17.6	12[c]	10^4-10^5
Paposo 425	425	25.02296	70.45019	19.6	17.4	9[c]	10^5-10^6

[a] WGS-84 datum
[b] estimated from a regression of weather station data in the region; see Quade et al. (2007)
[c] the Paposo sites are in coastal Lomas zone, and receive most of their moisture from frog, not included here
[d] from McKay et al. (2003); Warren and Rhodes (2006)

Table 2.

soil site	depth (cm)	carbonate (%)	$\delta^{13}C$ (‰) PDB	$\delta^{18}O$ (‰) PDB	NO_3 µmoles/gram soil	SO_4	PO_4	Cl
BAQ895	0-10	0.181	0.56	-1.15	4.6	335.571	BD	16.38
	10-20	0.787	1.17	-0.17	2.163	317.043	BD	12.778
	20-30	0.326	2.16	1.50	1.215	206.924	BD	8.539
	30-40	0.346	2.43	0.34	1.268	323.724	BD	10.236
	40-50	0.205	1.05	0.27	1.388	352.511	BD	16.55
BAQ1370	0-10	2.183	2.23	-1.46	1.835	253.264	BD	4.344
	10-20	0.711	2.28	-0.73	17.14	412.014	BD	35.355
	20-30	0.227	-0.16	-3.63	67.67	428.253	BD	97.896
	30-40	0.076	-3.42	-3.48	84.94	483.94	BD	107.275
	40-50	0.064	-0.69	0.30	162.09	463.956	BD	148.571
BAQ1552	0-10	0.354	4.07	-2.42	0.749	9.898	BD	2.081
	10-20	1.395	5.26	1.58	0.678	28.804	BD	1.771
	20-30	1.767	4.72	0.53	0.894	99.633	BD	1.499
	30-40	2.305	4.06	0.20	1.515	168.295	BD	2.862
	40-50	0.682	1.93	-1.61	14.939	382.947	BD	13.745
BAQ2420	0-10	2.782	-4.31	-7.55	0.395	0.865	BD	3.571
	10-20	2.569	-5.37	-7.64	0.253	0.815	BD	1.138
	20-30	2.872	-6.19	-8.43	0.374	1.156	BD	1.7
	30-40	2.809	-5.78	-7.08	0.157	1.291	BD	0.866
	40-50	2.988	-6.62	-8.10	0.262	1.098	BD	1.344
BAQ2462	0-10	2.803	1.54	-3.07	0.369	2.626	BD	4.187
	10-20	2.295	1.90	-1.10	0.366	4.757	BD	5.571
	20-30	2.878	1.78	-0.46	0.573	3.087	BD	6.713
	30-40	3.187	1.74	1.83	0.669	1.798	BD	6.349
	40-50	2.674	2.87	2.59	0.358	1.668	BD	6.3
BAQ2838	0-10	0.072	4.94	0.21	0.338	2.831	BD	1.817
	10-20	0.240	4.58	1.70	0.202	2.017	BD	1.617
	20-30	0.165	3.32	2.79	0.165	0.801	BD	1.285
	30-40	0.079	2.60	1.33	0.339	0.863	BD	2.497
	40-50	0.136	3.57	4.51	0.278	0.926	BD	1.412
BAQ2687	0-10	0.357	0.81	3.34	0.329	0.451	BD	0.763
	10-20	1.819	-2.15	2.52	0.144	0.191	BD	2.151
	20-30	3.584	-0.99	3.29	0.127	0.209	BD	0.585
	30-40	1.804	-5.71	0.31	0.137	0.291	BD	1.447
	40-50	1.457	-2.52	2.32	0.128	0.241	BD	0.811
BAQ3473	0-10	BD	BD	BD	0.91	75.321	BD	2.454
	10-20	BD	BD	BD	0.792	2.698	BD	2.153

	20-30	BD	BD	BD	0.934	2.785	BD	1.276
	30-40	BD	BD	BD	0.372	27.183	BD	0.887
	40-50	BD	BD	BD	0.378	34.998	BD	0.701
BAQ4166	0-10	BD	BD	BD	1.623	0.468	BD	1.073
	10-20	BD	BD	BD	0.812	0.262	BD	0.969
	20-30	BD	BD	BD	0.463	0.195	BD	0.662
	30-40	BD	BD	BD	0.387	0.224	BD	1.411
	40-50	BD	BD	BD	0.437	0.27	BD	2.844
BAQ4697	0-10	BD	BD	BD	0.436	0.336	BD	0.785
	10-20	BD	BD	BD	0.54	0.376	BD	0.773
	20-30	BD	BD	BD	0.304	0.261	BD	1.093
	30-40	BD	BD	BD	0.302	0.308	BD	1.218
YUN2029	0-10	BD	BD	BD	0.2681	0.8766	BD	0.8646
	10-20	BD	BD	BD	0.3221	0.8899	BD	1.6076
	20-30	BD	BD	BD	0.4811	0.9226	BD	1.3775
	30-40	1.160	4.55	8.02	38.2032	82.1382	BD	15.992
	40-50	5.466	4.32	6.52	57.2467	145.1651	0.1819	18.4636
YUN1005	0-10	0.315	5.68	1.11	0.5046	320.7584	BD	2.0662
	10-20	1.479	5.67	0.10	1.3331	327.8238	BD	2.5094
	20-30	1.532	3.87	0.44	3.1576	334.7359	0.366	9.1426
	30-40	1.989	3.17	-0.99	8.4895	345.6264	BD	29.6357
	40-50	1.732	3.24	-0.57	16.8846	348.0026	BD	58.4322
YUN1242	0-10	BD	BD	BD	0.8353	4.1166	0.1453	4.9903
	10-20	0.196	3.68	2.30	3.5858	6.3197	0.2537	28.1346
	20-30	2.551	3.05	0.43	2.6572	5.2542	BD	21.8526
	30-40	3.142	3.84	1.68	2.5503	16.7441	BD	14.9937
	40-50	1.211	3.78	1.29	3.6813	368.4969	0.29	22.1711
YUN1609	0-10	0.081	4.27	-2.17	0.4375	6.218	BD	2.4275
	10-20	1.582	5.23	1.57	0.3571	5.7065	BD	1.825
	20-30	1.566	4.22	1.14	1.4556	29.402	BD	1.9887
	30-40	1.814	3.76	0.32	15.2799	102.2739	0.2371	18.9885
	40-50	1.858	2.29	-0.84	25.2363	462.4015	BD	27.0852
YUN3184	0-10	0.686	6.56	2.65	0.8189	359.6316	0.3062	17.6632
	10-20	0.664	6.32	4.84	1.4337	336.5664	0.2406	2.2062
	20-30	1.056	5.79	4.52	1.8482	335.8791	0.4547	2.07
	30-40	0.627	2.66	6.22	0.1678	336.2982	0.2416	1.632
	40-50	0.758	2.64	4.09	1.7771	344.4832	0.2064	2.1779
YUN3153	0-10	0.422	5.62	6.47	0.2362	35.6588	BD	2.2789
	10-20	0.138	5.14	5.84	0.2448	334.8696	0.3246	2.3641
	20-30	BD	5.17	6.90	0.2899	349.8186	0.2881	1.4475
	30-40	BD	BD	BD	0.2473	353.942	0.3051	0.9879
	40-50	BD	BD	BD	0.3804	369.2308	0.3761	1.4869
YUN3259	0-10	0.278	4.50	1.62	0.0946	0.4888	BD	1.3431

	10-20	0.812	1.43	-1.16	0.1465	0.6061	BD	2.252
	20-30	0.796	-0.87	-3.00	0.1261	0.5939	BD	3.0713
	30-40	0.698	-0.51	-1.95	0.1028	0.4872	BD	2.1364
	40-50	0.667	BD	BD	0.1034	0.3906	BD	1.3603
YUN3346	0-10	BD	BD	BD	0.145	0.5373	BD	4.8279
	10-20	BD	BD	BD	0.1147	0.4961	BD	1.5464
	20-30	BD	BD	BD	0.126	0.5474	BD	1.3625
	30-40	BD	BD	BD	0.109	0.4712	BD	0.5618
	40-50	BD	BD	BD	0.149	0.8009	BD	2.1924
YUN3428	0-10	BD	BD	BD	0.1658	0.3841	BD	1.9863
	10-20	BD	BD	BD	BD	0.3551	BD	2.1866
	20-30	BD	BD	BD	0.097	0.3412	BD	0.68
	30-40	BD	BD	BD	0.1289	0.3859	BD	1.3341
	40-50	BD	BD	BD	0.1175	0.3988	BD	0.8609
YUN3533	0-10	BD	BD	BD	BD	0.2744	BD	0.5217
	10-20	BD	BD	BD	BD	0.3275	BD	0.877
	20-30	BD	BD	BD	0.1457	0.3292	BD	0.951
	30-40	BD	BD	BD	0.1787	0.4393	0.3083	0.6337
	40-50	BD	BD	BD	0.1417	0.3892	BD	2.3533
YUN3856	0-10	BD	BD	BD	0.2827	0.314	BD	1.2316
	10-20	BD	BD	BD	0.1484	0.2562	BD	1.2328
	20-30	BD	BD	BD	0.1267	0.392	BD	1.4065
	30-40	BD	BD	BD	0.2247	0.9062	BD	1.8617
	40-50	0.116	BD	BD	0.0975	8.8504	BD	2.8507